Published in final edited form as:
Free Radic Biol Med. 2007 May 15; 42(10): 1470–1480.

Mitochondrial alterations in livers of *Sod1*$^{-/-}$ mice fed alcohol

Irina G. Kessova and **Arthur I. Cederbaum**
Department of Pharmacology and Biological Chemistry, Mount Sinai School of Medicine, New York, NY 10029, USA

Abstract

Chronic alcohol consumption induced liver injury in Cu, Zn-superoxide dismutase –deficient mice (*Sod1*$^{-/-}$) with extensive centrilobular necrosis and inflammation and a reduction of hepatic ATP content. Mechanisms by which ethanol decreased ATP in these mice remain unclear. We investigated alterations in mitochondria of *Sod1*$^{-/-}$mice produced by chronic ethanol treatment. These mitochondria had an increase in state 4 oxygen consumption with succinate and especially with glutamate plus malate compared to pair-fed *Sod1*$^{-/-}$mice or mitochondria from wild type mice fed dextrose or ethanol. This uncoupling was associated with a decrease in ADP/O and respiratory control ratios, a decline in mitochondrial membrane potential, enhanced mitochondrial permeability transition and decreased aconitase activity. Total thiols and uncoupling protein 2 levels were elevated in the pair-fed *Sod1*$^{-/-}$mitochondria, perhaps an adaptive response to oxidant stress. However, no such increases were found with the ethanol-fed *Sod1*$^{-/-}$mitochondria suggesting a failure to develop these adaptations. The mitochondria from the ethanol-fed *Sod1*$^{-/-}$mice had elevated levels of cleaved Bax, Bak, Bcl-xl and adenine nucleotide translocator. Immunoprecipitation studies revealed increased association of Bax and Bak with the adenine nucleotide translocator. ADP-ATP exchange was very low in the ethanol-fed *Sod1*$^{-/-}$mitochondria. These results suggest that ethanol treatment of *Sod1*$^{-/-}$mice, produces uncoupling and a decline in $\Delta\psi$, swelling, increased association of proapoptotic proteins involved in the permeability transition and decreased adenine nucleotide translocator activity, which may be responsible for the decline in ATP levels and development of necrosis in this model of alcohol-induced liver injury.

Keywords

Alcohol induced liver disease; Cu; Zn- superoxide dismutase; knockout mice; mitochondria; oxidative stress

Introduction

Mitochondria play a key role in controlling the energy balance and in signaling of either a cell survival or death response, or whether mitochondrial injury results in apoptosis or necrosis. Mitochondria represent the major intracellular source of ROS especially superoxide radical, which is generated as a byproduct of oxygen consumption by the respiratory chain. Oxidative stress appears to play a central role in mechanisms by which ethanol is hepatotoxic (1). Damage to the mitochondria and increased production of ROS by mitochondria after ethanol treatment

Corresponding author: Dr.Arthur I. Cederbaum, Department of Pharmacology and Biological Chemistry, Box 1603, Mount Sinai School of Medicine, One Gustave L. Levy Place, New York, NY 10029, Ph: (212) 241-7285, Fax: (212) 996-7214, E-mail: Arthur.Cederbaum@mssm.edu

may contribute to ethanol-induced oxidative stress (2–5). Acute ethanol treatment of rat hepatocytes increased ROS production in mitochondria, produced depolarization of the mitochondrial membrane which resulted in a mitochondrial permeability transition (MPT) and caused Bax translocation from cytosol to mitochondria; these effects led to subsequent formation of Bax-VDAC complexes, release of cytochrome c, caspase 3 activation, and apoptosis (6–8). Chronic alcohol consumption induced inhibition of complexes I and III of the mitochondrial electron transport chain, impaired the rate of ATP synthesis, decreased levels of ATP and increased ROS production in rat liver (9,10). Mitochondria isolated from rats chronically fed ethanol exhibited a markedly increased sensitivity to MPT induction caused by a variety of agents implicated in both necrotic (Ca^{2+}) and apoptotic (ceramide, GD3 ganglioside, and Bax) forms of cell death (11). Ethanol promotes oxidative stress in mitochondria, both by increasing ROS formation and by decreasing mitochondrial defense mechanisms. Mitochondrial GSH was depleted by an ethanol-induced impairment in mitochondrial GSH transport, due to decreased membrane fluidity (12). Patients and baboons with alcoholic hepatitis displayed mitochondria with morphological aberrations (13–15). While the role of oxidative stress in alcohol-induced cell injury is well documented (16), what alterations occur in mitochondria in *in vivo* models with alcohol-induced liver injury are still uncertain.

It has been difficult to study mechanisms responsible for alcohol-induced liver injury since oral administration of ethanol in liquid diets, while producing steatosis and oxidant stress in the liver, does not cause liver necrosis or fibrosis. There is a need for new oral models of ethanol treatment that results in the development of liver injury. Because alcoholic liver injury has been linked to oxidative stress, we reasoned that a compromised antioxidant defensive system in the liver could exaccerbate liver injury produced by ethanol. Several studies have shown a decrease in SOD1 activity in rat liver after alcohol treatment (17,18) and adenoviral delivery of SOD1 protected against liver injury caused by alcohol (19). A model of chronic alcohol-induced liver injury using Cu, Zn-superoxide dismutase –deficient mice (*Sod1*$^{-/-}$*) was developed (*20). Feeding the homozygous *Sod1*$^{-/-}$mice with ethanol (10% of total calories) for 3 weeks resulted in extensive centrilobular necrosis and inflammation and increased carbonyls, lipid peroxidation aldehydic products and 3-nitrotyrosine protein adducts, indicative of enhanced oxidative and nitrosative stress. Since liver injury was accompanied by reductions of hepatic ATP content, mitochondrial GSH levels and activity of the Mn-SOD, we suggest that the increased mitochondrial oxidative stress and subsequent alterations in mitochondria caused by chronic alcohol may be important in the mechanisms of this liver injury. The goal of this study was to evaluate mitochondrial function in livers of *Sod1*$^{-/-}$mice chronically fed ethanol, especially as it may relate to MPT sensitivity.

Materials and Methods

Mice

Cu,Zn–superoxide dismutase deficient by targeted mutation mice (B6; 129S7-*Sod1* ^{tm1Leb}) were purchased from Jackson Laboratories (Bar Harbor, Maine) and bred at the animal facility at Mount Sinai School of Medicine. All mice were cared for according to the NIH *Guide for the Care and Use of Laboratory Animals.* Mice were genotyped at 1month of age by polymerase chain reaction (PCR). Genomic DNA isolated from mouse tail was digested overnight in tail tip buffer containing 0.1 mM EDTA, 0.5 % SDS, Proteinase K (1 mg/ml), 50 mM Tris-HCl, pH 8.0. DNA was isolated by a chloroform/phenol procedure. The targeted allele was detected as a 250-bp fragment (HPRT) using primers IMR0781(5′-TGTTCTCCTCTTCCTCATCTCC-3′) mouse Pgk promoter forward primer for the PgkHPRT minigene and IMR0782 (5′-ACCCTTTCCAAATCCTCAGC-3′) as HPRT exon 2 reverse primer for the PgkHPRT minigene. The wild type allele was detected as a 123bp fragment

using primers IMR0878 (5′-TGAACCAGTTGTGTTGTCAGG-3′) and IMR0888 (5′-TCCATCACTGGTCACTAGCC-3′). The 25 μl PCR reaction mixture contained Ready-To-Go™ PCR Beads, 300 ng DNA and 0.3 μM of each primer. The PCR conditions used were one cycle of denaturation at 94°C for 3min, followed by 12 cycles of denaturation at 94°C for 30 sec, annealing at 61°C for 30 sec and extension at 72°C for 35 sec, followed by 25 cycles at 94°C for 20 sec, at 58°C for 30 sec, at 72°C for 35 sec and a final cycle at 72°C for 5 min. Homozygous (*Sod1*$^{-/-}$) and wild type (*Sod1*$^{+/+}$) mice at age of 2 month were fed the ethanol diet at 10% of total calories for the first week and 20 % ethanol for the second week while control groups were pair-fed the control dextrose diet.

Mitochondrial isolation

After 2 weeks on the respective diets, the mice were sacrificed with an overdose of pentobarbital and livers were rapidly dissected in ice cold 0.25 mM sucrose. Two weeks of treatment were used in this study since severe liver injury occurs after 3 weeks of feeding alcohol to the SOD1 knockouts and we were interested in evaluating whether mitochondrial dysfunction occurs prior to the development of this severe injury. All procedures were carried out at 4°C. Livers were minced in fresh sucrose-based medium (250 mM sucrose, 1 mM $MgCl_2$, 0.1 mM EGTA, 20 mM HEPES, pH 7.4) and gently homogenized manually (w/v) using a tissue grinder with loose-fitting pestle. The resulting homogenate was centrifuged at 800 × g for 5 min twice, and the supernatant fraction was centrifuged at 9,000 × g for 10 min to obtain the mitochondrial pellet. This pellet was washed with isolation medium (EGTA free for MPT measurements) and centrifuged at 10,000g for 10 min. The final pellet was homogenized in the above buffer. Protein concentration was measured by the DC protein Assay Kit II (Bio-Rad, Hercules, CA). To assure equivalent yield and purity of the mitochondria isolated from the 4 groups of mice, porin levels per mg mitochondrial protein were determined by Western blot analysis.

Determination of aconitase activity

The activity of aconitase in the mitochondrial fractions was measured by the conversion of citrate to α-ketoglutarate coupled to the reduction of $NADP^+$. Aconitase activity was monitored for 3–5 min by determining the absorbance at 340nm in freshly prepared 50 mM Tris-HCl buffer containing 0.2 mM $NADP^+$, 30 mM sodium citrate, 2 unit/ml of isocitrate dehydrogenase, and 0.6 mM $MnCl_2$. Mitochondrial pellets were suspended in 2 mM sodium citrate buffer, 0.6 mM $MnCl_2$, 1 mM sodium succinate and solubilized by repeating a freezing-thawing cycle 3 times. The reaction was started by adding the mitochondria samples. Aconitase activity is defined as the amount of enzyme necessary to catalyze the formation of 1 nmol of isocitrate/min at 37 °C.

Thiols and Sulfide

Total mitochondrial thiols were assayed using the Thiol and Sulfide Quantitation Kit (Molecular Probes, Carlsbad, CA), which provides an ultrasensitive colorimetric assay for quantitating both protein and nonprotein thiols. The nonprotein thiols essentially reflect GSH levels in the isolated mitochondria. In this assay thiols reduce a disulfide inhibited derivative of papain, stoichiometrically releasing the active enzyme. Proteins are denatured such that all protein thiols are accessible: the combination of nonprotein thiols plus protein thiols reduce the papain disulfide prosubstrate to the active reduced sulfhydryl form of papain and catalytic activity is proportional to the total free thiols available to reduce the papain disulfide prosubstrate. The activity of the papain is then measured using the chromogenic papain substrate, *N*-benzoyl-L-arginine, *p*-nitroanilide (L-BAPNA) according to kit instructions. Validation of this assay was shown by the lack of formation of p-nitroaniline with GSSG as compared to GSH, inhibition of p-nitroaniline formation when the mitochondrial extract was

treated with diethylmaleate to bind free thiol groups and finding similar results when Ellman's reagent was used to assay free thiol groups.

O2 consumption

Respiratory rates were assessed by measuring the oxygen consumption of mitochondria using Clark-type electrodes in 3 ml sealed Perspex chambers, which were continuously magnetically stirred at 30°C. Mice liver mitochondria (0.8mg/ml) were incubated in respiration buffer composed of 120 mM KCl, 3 mM HEPES, 1 mM EGTA, 25 mM sucrose, 5 mM $MgCl_2$, 5 mM KH_2PO_4 at pH 7.4 in the presence of either 5 mM malate plus 5 mM glutamate or 15 mM succinate plus 2.7 uM rotenone as substrates to measure state 4 respiration. State 3 respiration was measured after the addition of ADP at a final concentration of 0.3 mM.

Spectrofluorometric measurements of Δψ

The electrical potential across the inner mitochondrial membrane ($\Delta\psi$) was estimated by monitoring of fluorescence quenching of Rhodamine 123 (21). Fluorescence with excitation at 503 nm (2.5 nm slit) and emission at 527 nm (3 nm slit) was measured in a buffer containing 150 mM sucrose, 5 mM $MgCl_2$, 2.7 μM rotenone; 0.2 μM Rhodamine 123; 5 mM KPi buffer; 20 mM potassium-HEPES buffer at pH 7.4 and mitochondria (0.167mg/ml). After incubation for 2–3 min, respiratory substrate disodium succinate (5 mM) was added to initiate state 4 respiration and then 300 μM ADP was added to initiate state 3 respiration. To de-energize the mitochondria, an uncoupler (1.3 μM CCCP) and respiratory inhibitor (1.3 μg/ml antimycin) were added. Rhodamine was dissolved in ethanol and its concentration was assayed spectrophotometrically at 507 nm (€507=101mM-1 cm^{-1}). The ethanol concentration in all incubation mixtures was kept below 0.4% (v/v).

Measurement of mitochondrial permeability transition

Mitochondria (0.5mg/ml) were incubated in the buffer used above for oxygen consumption at 25° C. 1mM glutamate and 1mM malate were added as respiratory substrates. MPT was induced in mitochondria by addition of either 10, 50, or 150 μM $CaCl_2$. 2 μM cyclosporin A was added before incubation as a control to prevent the MPT. Swelling was monitored every minute over a 30 min incubation by absorbance at 540 nm.

Detection of cytochrome c release

Mitochondria (1 mg of protein/ml) were incubated for 15 min at 25 °C in respiration buffer with the indicated additions. The reaction mixtures were then centrifuged at 13,000 × g for 10 min at 4 °C to obtain the mitochondrial pellets. The supernatant fractions were further spun at 100,000 × *g* for 15 min at 4 °C to eliminate mitochondrial membrane fragments and concentrated by ultrafiltration through Centricon 10 membranes (Millipore, Billerica, MA) at 4 °C. The concentrated supernatants were subjected to 18% SDS-PAGE, transferred to 0.2μm nitrocellulose membranes and analyzed by Western blotting using anti-cytochrome c antibody.

ADP/ATP translocase activity

Liver mitochondria were suspended (7mg/500μl) in 0.6 M mannitol, 0.2%BSA, 10 mM MOPS, and 0.1 mM EDTA at pH 6.8. Mitochondria were incubated with 15 μl of [^{3}H] ATP (40Ci/mmol) for 45 min at 4°C in the presence or absence of 100 μM atractyloside. Mitochondria were washed twice to eliminate free [^{3}H] ATP. The ADP-ATP exchange was initiated by addition of cold ADP (standard concentration of 400 μM) and stopped by addition of 100 μM atractyloside after 10 sec. The reaction mixtures were then centrifuged at 9,000 × g for 10 min at 4 °C to obtain the mitochondrial pellets. Supernatant and mitochondrial pellets were subjected to scintillation counting. ATP release into the 9000 × g supernatant fraction was

measured and expressed as a percentage of [^{3}H] counts compared to [^{3}H] counts in control mitochondria.

Western blotting, protein cross-linking and immunoprecipitation

In vivo cross-linking for ANT interactions with proteins of the Bcl2 family and VDAC was performed with dimethyl 3,3′-dithio-bis(proprionate)x2HCl (DTBP) (Pierce Biotechnology, Inc., Rockford, IL). Mitochondria were treated with 2 mM of cross-linkers in PBS for 30 min at room temperature. After the reaction was quenched with 50 mM Tris-HCl for 10 min at 4° C, mitochondria were washed in PBS. Mitochondria were then lysed with lysis buffer : 10 mM Tris-HCl, pH 7.4, 142.5 mM KCl, 5 mM $MgCl_2$, 1 mM EDTA, 1 mM PMSF, with 0.5% Nonidet P-40, and 20 μM leupeptin for 30 min on ice and centrifuged to remove insoluble debris. Immunoprecipitation was carried out as follows. Samples were precleared by mixing with control IgG protein and Protein G Plus-Agarose beads (Santa-Cruz Biotechnology, SantaCruz, CA) for 60 min at 4°C in a rocker, and the beads were removed by centrifugation. The resultant supernatants were incubated with anti-ANT antibodies (2 μg/ml) at 4°C for 2 h. Immunoprecipitates were collected by incubating with protein G-Sepharose for 60 min, followed by centrifugation for 2 min at 4°C. The pellets were washed with lysis buffer three times. After the final wash, the beads were suspended in SDS-sample buffer, and the samples were analyzed by SDS-PAGE and Western blotting.

Determination of caspase 3 activity

Caspase 3 activity in hepatic cytosols was assayed using the fluoregenic peptide 50 μM Ac-DEVD-AMC. The assay was carried out using 200 μg of cytosolic protein in a total volume of 100 μl. Following incubation in assay buffer at 37 °C for 30 min, the reaction was quenched by addition of 500 μl cold ethanol. A 2.0-ml aliquot of H_2O was then added and the fluorescence of the samples was evaluated at 360/460 nm using a Bio-Tek Kontron SFM 25 spectrofluorimeter. Peptidase activities were measured in the absence and presence of the caspase 3 inhibitor Ac-DEVD-CHO (50μM); the difference between the two rates was attributed to the caspase -3 activity. The results were expressed as arbitrary units of fluorescence per milligram of protein.

Terminal Deoxynucleotidyl Transferase–Mediated dUTP Nick-End Labeling

DNA fragmentation was assessed via terminal deoxynucleotidyl transferase–mediated dUTP nick-end labeling (TUNEL) assay using the ApopTag *in situ* apoptosis detection kit (Serological Corp., Atlanta, GA). The quantitative analysis of positive nuclei with DNA fragmentation was performed by counting the average number of stained nuclei per visual field (original magnification × 400).

Statistics—Two-way analysis of variance (ANOVA) followed by Bonferroni post-hoc test was used for the determination of statistical significance of the experimental results.

Results

Oxidative stress in mitochondria of Sod1$^{-/-}$ mice

In order to evaluate oxidative stress in mitochondria of mice, we examined mitochondrial aconitase activity, a Fe-S cluster enzyme that is inactivated by superoxide and peroxynitrite. Inactivation of aconitase activity is believed to be a reliable marker for mitochondrial superoxide production (22,23). Deletion of the *Sod1* gene caused 3.3- fold-decline in aconitase activity in liver of *Sod1*$^{-/-}$ mice fed dextrose (Fig. 1, A) Ethanol administration caused a 50% decrease in enzyme activity in mitochondria of the knockout mice and a 30% decrease in wild type mice. These results suggest that, the superoxide production in mitochondria of *Sod1*$^{-/-}$

mice is high and can be further increased with alcohol consumption. Because ROS oxidize thiol groups, we measured the concentration of protein-associated and low molecular weight thiols (mainly GSH) in mitochondria (Fig. 1B). The content of reduced thiols in mitochondria of *Sod1* knockout mice was increased 2-fold compared with wild type mice, possibly an adaptive mechanism to oxidative stress. However, ethanol administration produced a decline in thiol content in mitochondria of *Sod1*$^{-/-}$ mice. No effect by ethanol was seen in mitochondria from the wild type mice (Fig. 1B). Interestingly, the pattern of changes in total thiol content in mitochondria of knockout mice produced by alcohol is similar to the changes in mitochondrial GSH content which were detected in our previous study i.e. an increase in the mitochondria from the *Sod1*$^{-/-}$ mice fed dextrose and a decrease after chronic ethanol treatment (20). One of the protective mechanisms against ROS production in the matrix of mitochondria is a mild uncoupling of respiration and phosphorylation by activation of uncoupling proteins (UCP)(24). UCP2 content was increased in mitochondria of *Sod1*$^{-/-}$ mice fed dextrose compared with the other groups (Fig. 1C and D), perhaps like the increase in GSH and thiols an adaptive mechanism to inhibit matrix ROS production. However, chronic ethanol treatment caused a decline in UCP2 content in mitochondria of *Sod1*$^{-/-}$ mice that probably reflects a failure to adapt protection factors with increasing levels of oxidative stress. Porin levels per mg mitochondrial protein were identical in the 4 groups of mice suggesting equivalent yield and purity of the isolated mitochondria.

O_2 Consumption, Membrane potential

In the knockout mice, ethanol treatment increased the state 4 rate of oxygen consumption with glutamate plus malate as substrate, with no effect on state 3 rates of respiration (Tables 1). Respiratory control ratio values were decreased in *Sod1*$^{-/-}$ mice fed ethanol with either glutamate-malate or succinate as substrates due to the increase of state 4 respirations. A smaller increase in state 4 oxygen consumption was found with succinate as substrate (Table 1). Ethanol administration caused significant decreases in the ADP/O ratio for both glutamate-malate and succinate in *Sod1*$^{-/-}$ mice as compared with wild type mice fed ethanol (Table 1). The lower ADP/O ratio, and respiratory control ratio caused by ethanol in the *Sod1* knockouts, can probably be attributed to uncoupling of oxidative phosphorylation. With respect to the wild type mice, chronic ethanol treatment had little or no significant effects on these parameters (Table 1, 1). The electrochemical potential of the proton gradient generated across the mitochondrial membrane ($\Delta\psi$) was assessed by monitoring fluorescence quenching of Rh-123. Fig. 2 shows the effect of a series of additions on the dye fluorescence in isolated mitochondria of mice. Addition of succinate as a respiratory substrate to the medium containing mitochondria and Rh-123 decreased fluorescence, reflective of a high $\Delta\psi$ corresponding to state 4 of respiration. The decline in flourescence averaged 100,97, and 99 arbitrary units with mitochondria from the wild type mice fed dextrose or ethanol and the SOD1 knockout mice fed dextrose, respectively, whereas the decline averaged 49 arbitrary units with mitochondria from the SOD1 knockout mice fed ethanol. Quenching of Rh123 fluorescence by succinate in mitochondria of *Sod1*$^{-/-}$ mice fed alcohol was significantly less than it was in mitochondria of the other 3 groups of mice, indicating a reduction in $\Delta\psi$. Addition of ADP induced an enhancement of steady-state fluorescence, which corresponds to state 3 respiration, as the proton gradient significantly decreases due to its utilization to promote ADP phosphorylation. This enlargement of Rh123 fluorescence was lower in mitochondria of *Sod1*$^{-/-}$ mice compared with the other experimental groups (Fig. 2). The increase in fluorescence caused by addition of ADP averaged 31,32 and 30 arbitrary units for mitochondria from wild type mice fed dextrose or ethanol or from the SOD1 knockout mice fed dextrose, respectively but averaged only 9 arbitrary units with the mitochondria from the SOD1 knockout mice fed ethanol. Quenching of fluorescence was reversed by deenergization with the uncoupler CCCP and respiratory inhibitor antimycin. Taken as a whole, these data suggest uncoupling and a decline in $\Delta\psi$ in mitochondria of *Sod1*$^{-/-}$ mice fed ethanol.

Permeabilization of the mitochondrial membrane, Cytochrome c release

Depolarization of the inner mitochondrial membrane would be expected to accompany a significant opening of the MPT pore. Mitochondria isolated from wild type mice fed either dextrose or ethanol tolerated concentrations of 10 μM Ca^{2+} without undergoing the MPT as assessed by mitochondrial swelling (Fig. 3). At 50 μM and 150 μM Ca^{2+}, the mitochondria underwent the MPT and this was accompanied with cytochrome c release as presented in representative Western blots at the bottom of each figure. Ca^{2+}-induced MPT opening and cytochrome c release from mitochondria were inhibited by cyclosporin A. Mitochondria from *Sod1*$^{-/-}$ mice fed dextrose demonstrated a small degree of swelling and cytochrome c release without Ca^{2+} addition, while 50 μM and 150 μM Ca^{2+} increased swelling of mitochondria resulting in cytochrome c release as was seen with the wild type mitochondria (Fig. 3C). Chronic ethanol consumption further increased induction of the MPT in mitochondria even without any addition of Ca^{2+}causing significant cytochrome c release. In addition, alcohol sensitized the mitochondria to MPT induction at 10 μM Ca^{2+} (Fig. 3D), a calcium concentration which did not induce the MPT in the other 3 groups. Cyclosporin A partially inhibited this Ca^{2+}-induced MPT as well as cytochrome c release from mitochondria of *Sod1*$^{-/-}$ mice chronically fed ethanol.

The content of Bcl-2 family proteins in mitochondria and their association with ANT

For further evaluation of uncoupling of respiration and phosphorylation as well as the increase of nonspecific pore opening in mitochondria of *Sod1*$^{-/-}$ mice fed ethanol, the content of Bcl-2 family proteins were evaluated by SDS–PAGE and immunoblotting with the corresponding antibodies. Their possible association with ANT was also studied. We detected the 21kD form of Bax, a proapoptotic member of the Bcl-2 family in mitochondria of wild type mice fed dextrose or ethanol whereas the cleaved 19kD form of Bax (which is able to oligomerize) was observed in mitochondria of both knockout mice (Fig. 4A). Ethanol consumption produced a 3–fold increase in the content of cleaved Bax as compared with the Bax level in mitochondria of *Sod1*$^{-/-}$ mice fed dextrose (Fig. 4). Increased levels of another proapoptotic protein, Bak, were detected in mitochondria of *Sod1*$^{-/-}$ mice fed ethanol (Fig. 4A). Levels of the antiapoptotic Bcl-xl were also higher in the *Sod1*$^{-/-}$ mice fed ethanol, as were levels of ANT. The content of VDAC was not significantly changed in any of the groups. Chronic ethanol treatment had no effect on Bax, Bak Bcl-xl, VDAC or ANT protein levels in the wild type mice. Besides total levels of these proteins, their association with ANT was evaluated since ANT is one of the critical proteins regulating the MPT. After immunoprecipitating ANT from the mitochondria of the 4 groups, possible associated proteins were evaluated by Western blotting. Chronic ethanol feeding of the *Sod1*$^{-/-}$ mice caused an increase in levels of Bax and Bak but not Bcl-xl or VDAC in the ANT immunoprecipitate (Fig. 4 ANT-IP).

ANT activity

The content of ANT protein was elevated in the mitochondria of *Sod1*$^{-/-}$ mice fed ethanol (Fig. 4A). To investigate functional activity of ANT, we measured ADP/ATP exchange in the isolated mitochondria. Ethanol feeding significantly reduced ADP/ATP translocation through the mitochondrial membrane of *Sod1*$^{-/-}$ mice, as compared with the other 3 groups of mice (Fig. 5).

DNA fragmentation and Caspase-3 activity

TUNEL results showed that there were more hepatocytes with positive staining nuclei in *Sod1*$^{-/-}$ mice fed ethanol (4.5 ± 0.9; per visual field of approximately 100 cells) than in the *Sod1*$^{-/-}$ mice fed dextrose (1.4 ± 0.3). No TUNEL staining was observed in the wild type mice fed ethanol or dextrose (Fig. 6A). Caspase-3 activity showed a significant increase in *Sod1*$^{-/-}$ mice fed dextrose compared to the alcohol-fed *Sod1*$^{-/-}$ mice and wild type mice fed

dextrose or ethanol (Fig. 6B). These results with caspase-3 activity suggest that TUNEL reflects DNA fragmentation largely due to non-specific damage rather than apoptosis. Chronic ethanol feeding potentiates liver injury in the *Sod1*$^{-/-}$ mice however, this combined injury by ethanol in *Sod1* knockout mice is primarily necrotic (20).

Discussion

Ethanol has long been known to inhibit mitochondrial oxygen consumption and ATP production (2,5,8). While this is thought to play a role in alcohol-induced liver injury, most studies showing impairment of mitochondrial functions occur in models which do not exhibit significant liver injury beyond steatosis. A recent study reported that unlike results with rat liver mitochondria, chronic ethanol feeding had no significant effect on mouse liver mitochondrial oxygen uptake (25) a result confirmed in the current study with the wild type Sod1 positive mice fed ethanol. Thus the role of mitochondrial dysfunction, while likely and logically believed to be important in alcohol-induced liver injury, remains unclear and not proven.

We have previously shown that chronic ethanol feeding produced liver injury in mice lacking SOD1 (20). This model provides an oral alcohol feeding model which produces significant liver injury and lends some support for the overall hypothesis that oxidative stress plays a role in alcohol-induced toxicity to the liver. Hepatic ATP levels and mitochondrial GSH and SOD2 activity were lower in the ethanol-treated SOD1 knockout mice leading to the suggestion that mitochondrial damage may play an important role in the overall toxicity produced by ethanol in this model. The goal of the current study was to directly evaluate whether chronic alcohol treatment of SOD1 knockout mice indeed does produce mitochondrial injury. In this study, chronic ethanol administration was shown to intensify oxidative changes in mitochondria of *Sod1*$^{-/-}$ mice. There was an apparent increase in superoxide production in mitochondria of *Sod1* knockout mice as reflected by inactivated aconitase activity. To cope with oxidative stress, mitochondria of *Sod1*$^{-/-}$ mice up-regulated some adaptive defensive responses such as an increase of total thiols, GSH and UCP2 protein content. Thiols, including glutathione are protective antioxidants, acting as free radical scavengers, therefore thiol-disulfide balance can be an indication of oxidative damage in tissues. The increase of UCP2 proteins is believed to occur during mild oxidative stress to cause some uncoupling due to lowering of the proton motive force, with a subsequent decrease in superoxide production (24). However, despite some adaptive mechanisms against oxidative stress, mitochondria of mice with deletion of the SOD1 enzyme and fed the dextrose diet still showed spontaneous swelling and MPT opening even in the absence of added Ca^{2+}, some cytochrome c release, caspase-3 activation and apoptosis in liver tissue. These data confirm the important role of SOD1 in superoxide dismutation and protection of mitochondria from oxidative stress. Indeed, recent studies showed that SOD1 is localized in mitochondria (26,27), and by protecting mitochondria from ROS-induced injury SOD1 could determine the fate of cells (28). A recent study showed that mitochondrial SOD1 was released from mitochondria in parallel to cytochrome c release, consequently increasing the susceptibility of mitochondria to oxidative stresses, induction of ANT oxidation, and the opening of MPT pores and eventually leading to the development of apoptotic reactions (29).

Chronic ethanol consumption increased oxidative stress as revealed by the further inactivation of aconitase activity and the decline in the adaptive enlargement of total thiol and UCP2 contents in mitochondria of *Sod1*$^{-/-}$ mice. In rats, chronic alcohol consumption induced inhibition of complexes I and III of the electron transport chain of the rat liver mitochondria and impaired the rate of ATP synthesis (9). We did not detect any significant decreases in the rate of respiration in mitochondria of wild type and knockout mice by ethanol as found with rat liver mitochondria. This possible species difference in sensitivity of mitochondrial

respiration to ethanol has also been reported by others (30). However, ethanol enhanced the uncoupling of respiration and oxidative phosphorylation in mitochondria of *Sod1*$^{-/-}$ mice (but not in wild type mice) as detected by increased rates of respiration in state 4 and lowering of the respiratory control and the ADP/O ratio with glutamate plus malate as substrate. Quenching of Rh 123 fluorescence also showed that the mitochondria from the *Sod1*$^{-/-}$ mice did not utilize the $\Delta\psi$ efficiently as addition of ADP to these mitochondria did not elevate fluorescence, indicative of utilization of the $\Delta\psi$ to phosphorylate ADP to ATP, to the same extent as it did with mitochondria from the other 3 groups. The ethanol consumption increased MPT pore opening in mitochondria of *Sod1*$^{-/-}$ mice even in the absence of Ca^{2+}resulting in significant swelling and cytochrome c release as well as sensitizing the mitochondria to MPT opening at 10μM Ca^{2+}, a concentration without any effect in the other groups.

Since chronic alcohol consumption intensified swelling, uncoupled respiration and phosphorylation and produced a decline in membrane potential in mitochondria of *Sod1*$^{-/-}$ mice, the components of nonspecific pores (which regulate the MPT) were evaluated. The mitochondrial membrane permeability may be regulated by a so-called “megachannel,” whose composition is complex and controversial. The major proteins of these channels are the adenine nucleotide transporter (ANT) and the voltage dependent anion channel (VDAC) located at the contact sites of the inner and outer mitochondrial membrane (31,32). While VDAC levels were not altered by ethanol feeding, ANT levels were increased 2.5 fold in mitochondria from the SOD1 knockout mice. The exact role of the ANT in MPT is not clear as mitochondria from knockout mice lacking ANTs could still be induced to undergo the MPT although higher concentrations of calcium were required to initiate the MPT (33). It was concluded that ANTs are non-essential structural components of the MPT although they do contribute to its regulation (33). The MPT is characterized by an increase in the inner membrane permeability to compounds with molecular mass less than 1,500 daltons. MPT function can be modulated by members of the Bcl 2 family (31), e.g. mitochondria undergo general permeabilization upon their interaction with Bax or Bak proteins (34). Levels of Bax and Bak were elevated in the mitochondria from the ethanol-treated SOD1 knockout mice. It is known that the activation of Bax is mediated by the translocation of Bax from the cytoplasm to the mitochondria, where it undergoes cleavages to lower molecular weight forms. When cleaved, Bax can oligomerize and oligomerized Bax inserts into the mitochondrial outer membrane (35,36) where it can potentiate the MPT. A recent study using an *in vivo* model of apoptosis showed that there are apoptotic populations correspond to early, intermediate, and late apoptotic mitochondria, which are characterized by an increasing extent of permeabilization of their outer membrane and a gradual enrichment in oligomerized Bax proteins (37). We observed an increased level of Bax protein, and importantly of cleaved Bax in liver mitochondria of knockout mice fed ethanol. Bax has recently been reported to interact directly with the VDAC on the outer membrane to release cytochrome c, or with ANT on the inner membrane to initiate the permeability transition (31,32,38,39). During acute ethanol induced hepatocellular apoptosis, Bax, was shown to be translocated to the mitochondrial membrane before mitochondrial cytochrome *c* release, where it formed Bax/VDAC complexes (6–8). ROS generation in mitochondria was shown to oxidize critical thiol groups of ANT and to induce release of cytochrome c to initiate apoptosis (40). Thiol reductants (41,42) and oxidants (43,44) seem to regulate MPT by affecting the redox state of critical thiols relating to MPT pore formation. MPT occurs when thiol groups of inner membrane proteins including ANT are oxidized to induce conformational changes that form large nonselective pores. Indeed, cross-linking of inner membrane proteins was observed upon mitochondrial induction of the MPT (41,42,45). ANT is a bifunctional protein that, in physiological conditions, exchanges ATP and ADP on the inner mitochondrial membrane. Oxidation of Cys ^{160} and Cys ^{257} in ANT markedly increases the affinity of cyclophilin D to the Pro ^{62} residue of ANT, thereby inducing MPT (46). Pore formation by ANT would require a physical interaction with Bax. An increased association of Bax and Bak with ANT in mitochondria of *Sod1*$^{-/-}$ mice chronically fed with

ethanol was detected, perhaps due, in part, to the overall increased content of these components in the mitochondria of the ethanol-fed SOD1 knockout mice.. A dramatic decline of ADP/ATP translocase activity in these mitochondria was observed in spite of an increase of ANT levels. This suggests that the ANT has lost functional activity in these mitochondria, perhaps as a result of oxidation of critical cysteine residues. We suggest that increases in proapoptotic proteins such as Bax and Bak and their increased association with ANT could play role in permeabilizing the mitochondrial membrane, leading to the decline in $\Delta\psi$, RCR and ADP/O in mitochondria from *Sod1*$^{-/-}$ mice fed ethanol.

In tissue injuries due to ischemia/reperfusion, toxic chemicals, and viral infection, apoptotic and necrotic features often coexist, which can lead to cell killing either by apoptosis or necrosis (47–50). This process is described as “necrapoptosis”; and may begin with a common stress or death signal, proceed by shared pathways, but ultimately culminate in either cell lysis (necrosis) or programmed cellular resorption (apoptosis) depending on modifying factors; one important modifying factor is ATP (50). The liver injury produced by ethanol in *Sod1*$^{-/-}$ mice was mainly necrosis. We believe that the increase in TUNEL staining in the ethanol treated *Sod1*$^{-/-}$ mice reflects necrotic-induced DNA fragmentation rather than only apoptotic. Indeed, while some increase in caspase-3 activity was observed in the dextrose-fed *Sod1*$^{-/-}$ mice, compared to the wild type mice, this increase in caspase-3 activity was lower after the ethanol treatment which is not consistent with increased apoptosis. We previously reported that ATP levels were lowed by about 50% in livers of *Sod1*$^{-/-}$ mice fed ethanol (20). Hepatic ATP levels in the dextrose fed *Sod1*$^{-/-}$ mice were more then 80% wild type values (20). This switch of liver injury in *Sod1*$^{-/-}$ mice, from apoptosis to necrosis, by ethanol as reflected by lower caspase-3 activities may relate to the large decline in hepatic ATP level in the ethanol-treated knockout mice, a result of the uncoupling of respiration/oxidative phosphorylation and decline in mitochondrial membrane potential. The ANT interaction with proapoptoic proteins and its dysfunction as an ADP/ATP translocator in mitochondria of *Sod1*$^{-/-}$ mice as a consequence of chronic ethanol consumption may cause ATP depletion and necrosis, and thus contribute to the liver injury found in this model of ethanol toxicity.

Acknowledgements

These studies were supported by USPHS Grant AA06610 from The National Institute on Alcohol Abuse and Alcoholism.

References

1. Dey A, Cederbaum AI. Alcohol and oxidative liver injury. Hepatology 2006;43:S63–74. [PubMed: 16447273]
2. Bailey SM, Cunningham CC. Contribution of mitochondria to oxidative stress associated with alcoholic liver disease. Free Radic Biol Med 2002;32:11–16. [PubMed: 11755312]
3. Mansouri A, Gaou I, De Kerguenec C, Amsellem S, Haouzi D, Berson A, Moreau A, Feldmann G, Letteron P, Pessayre D, Fromenty B. An alcoholic binge causes massive degradation of hepatic mitochondrial DNA in mice. Gastroenterology 1999;117:181–190. [PubMed: 10381926]
4. Cahill A, Cunningham CC, Adachi M, Ishii H, Bailey SM, Fromenty B, Davies A. Effects of alcohol and oxidative stress on liver pathology: the role of the mitochondrion. Alcohol Clin Exp Res 2002;26:907–915. [PubMed: 12068261]
5. Bailey SM. A review of the role of reactive oxygen and nitrogen species in alcohol-induced mitochondrial dysfunction. Free Radic Res 2003;37:585–596. [PubMed: 12868485]
6. Adachi M, Higuchi H, Miura S, Azuma T, Inokuchi S, Saito H, Kato S, Ishii H. Bax interacts with the voltage-dependent anion channel and mediates ethanol-induced apoptosis in rat hepatocytes. Am J Physiol Gastrointest Liver Physiol 2004;287:G695–705. [PubMed: 15044178]

7. Higuchi HAdachi M, Miura SGores GJ, Ishii H. The mitochondrial permeability transition contributes to acute ethanol-induced apoptosis in rat hepatocytes. Hepatology 2001;34:320–328. [PubMed: 11481617]
8. Adachi M, Ishii H. Role of mitochondria in alcoholic liver injury. Free Radic Biol Med 2002;32:487–491. [PubMed: 11958949]
9. Bailey SM, Pietsch EC, Cunningham CC. Ethanol stimulates the production of reactive oxygen species at mitochondrial complexes I and III. Free Radic Biol Med 1999;27:891–900. [PubMed: 10515594]
10. Kukielka E, Dicker E, Cederbaum AI. Increased production of reactive oxygen species by rat liver mitochondria after chronic ethanol treatment. Arch Biochem Biophys 1994;309:377–386. [PubMed: 8135551]
11. Pastorino JG, Marcineviciute A, Cahill A, Hoek JB. Potentiation by chronic ethanol treatment of the mitochondrial permeability transition. Biochem Biophys Res Commun 1999;265:405–409. [PubMed: 10558880]
12. Colell A, Garcia-Ruiz C, Morales A, Ballesta A, Ookhtens M, Rodes J, Kaplowitz N, Fernandez-Checa JC. Transport of reduced glutathione in hepatic mitochondria and mitoplasts from ethanol-treated rats: effect of membrane physical properties and S-adenosyl-L-methionine. Hepatology 1997;26:699–708. [PubMed: 9303501]
13. Lieber CS, DeCarli L, Rubin E. Sequential production of fatty liver, hepatitis, and cirrhosis in sub-human primates fed ethanol with adequate diets. Proc Natl Acad Sci U S A 1975;72:437–441. [PubMed: 1054827]
14. Inagaki T, Koike M, Ikuta K, Kobayashi S, Suzuki M, Kato K. Ultrastructural identification and clinical significance of light microscopic giant mitochondria in alcoholic liver injuries. Gastroenterol Jpn 1989;24:46–53. [PubMed: 2707552]
15. Bruguera M, Bertran A, Bombi JA, Rodes J. Giant mitochondria in hepatocytes: a diagnostic hint for alcoholic liver disease. Gastroenterology 1977;73:1383–1387. [PubMed: 913978]
16. Cederbaum AI. Introduction-serial review: alcohol, oxidative stress and cell injury. Free Radic Biol Med 2001;31:1524–1526. [PubMed: 11744324]
17. Polavarapu R, Spitz DR, Sim JE, Follansbee MH, Oberley LW, Rahemtulla A, Nanji AA. Increased lipid peroxidation and impaired antioxidant enzyme function is associated with pathological liver injury in experimental alcoholic liver disease in rats fed diets high in corn oil and fish oil. Hepatology 1998;27:1317–1323. [PubMed: 9581686]
18. Zidenberg-Cherr S, Olin KL, Villanueva J, Tang A, Phinney SD, Halsted CH, Keen CL. Ethanol-induced changes in hepatic free radical defense mechanisms and fatty-acid composition in the miniature pig. Hepatology 1991;13:1185–1192. [PubMed: 2050333]
19. Wheeler MD, Kono H, Yin M, Rusyn I, Froh M, Connor HD, Mason RP, Samulski RS, Thurman RG. Delivery of the Cu/Zn-superoxide dismutase gene with adenovirus reduces early alcohol-induced liver injury in rats. Gastroenterology 2001;120:1241–1250. [PubMed: 11266387]
20. Kessova IG, Ho YS, Thung S, Cederbaum AI. Alcohol-induced liver injury in mice lacking Cu, Zn-superoxide dismutase. Hepatology 2003;38:1136–1145. [PubMed: 14578852]
21. Emaus RK, Grunwald R, Lemasters JJ. Rhodamine 123 as a probe of transmembrane potential in isolated rat-liver mitochondria: spectral and metabolic properties. Biochim Biophys Acta 1986;850:436–448. [PubMed: 2873836]
22. Hausladen A, Fridovich I. Superoxide and peroxynitrite inactivate aconitases, but nitric oxide does not. J Biol Chem 1994;269:29405–29408. [PubMed: 7961919]
23. Hausladen A, Fridovich I. Measuring nitric oxide and superoxide: rate constants for aconitase reactivity. Methods Enzymol 1996;269:37–41. [PubMed: 8791635]
24. Echtay KS, Murphy MP, Smith RA, Talbot DA, Brand MD. Superoxide activates mitochondrial uncoupling protein 2 from the matrix side. Studies using targeted antioxidants. J Biol Chem 2002;277:47129–47135. [PubMed: 12372827]
25. Venkatraman A, Shiva S, Wigley A, Ulasova E, Chhieng D, Bailey SM, Darley-Usmar V. The role of iNOS in alcohol-dependent hepatotoxicity and mitochondrial dysfunction in mice. Hepatology 2004;40:565–573. [PubMed: 15349894]
26. Kira Y, Sato EF; Inoue M. Association of Cu-Zn-type superoxide dismutase with mitochondria and peroxisomes. Arch Biochem Biophys 2002;399:96–102. [PubMed: 11883908]

27. Okado-Matsumoto A, Fridovich I. Subcellular distribution of superoxide dismutases (SOD) in rat liver: Cu,Zn-SOD in mitochondria. J Biol Chem 2001;276:38388–38393. [PubMed: 11507097]
28. Mondola P, Santillo M, Seru R, Damiano S, Alvino C, Ruggiero G, Formisano P, Terrazzano G, Secondo A, Annunziato L. Cu,Zn superoxide dismutase increases intracellular calcium levels via a phospholipase C-protein kinase C pathway in SK-N-BE neuroblastoma cells. Biochem Biophys Res Commun 2004;324:887–892. [PubMed: 15474511]
29. Li Q, Sato EF, Kira Y, Nishikawa M, Utsumi K, Inoue M. A possible cooperation of SOD1 and cytochrome c in mitochondria-dependent apoptosis. Free Radic Biol Med 2006;40:173–181. [PubMed: 16337891]
30. Venkatraman A, Shiva S, Davis AJ, Bailey SM, Brookes PS, Darley-Usmar VM. Chronic alcohol consumption increases the sensitivity of rat liver mitochondrial respiration to inhibition by nitric oxide. Hepatology 2003;38:141–147. [PubMed: 12829996]
31. Vyssokikh MY, Brdiczka D. The function of complexes between the outer mitochondrial membrane pore (VDAC) and the adenine nucleotide translocase in regulation of energy metabolism and apoptosis. Acta Biochim Pol 2003;50:389–404. [PubMed: 12833165]
32. Crompton M, Barksby E, Johnson N, Capano M. Mitochondrial intermembrane junctional complexes and their involvement in cell death. Biochimie 2002;84:143–152. [PubMed: 12022945]
33. Kokoszka JE, Waymire KG, Levy SE, Sligh JE, Cai J, Jones DP, MacGregor GR, Wallac DC. The ADP/ATP translocator is not essential for the mitochondrial permeability transition pore. Nature 2004;427:461–465. [PubMed: 14749836]
34. Degli Esposti M, Dive C. Mitochondrial membrane permeabilisation by Bax/Bak. Biochem Biophys Res Commun 2003;304:455–461. [PubMed: 12729579]
35. Green DR, Kroemer G. The pathophysiology of mitochondrial cell death. Science 2004;305:626–629. [PubMed: 15286356]
36. Khosravi-Far R, Esposti MD. Death receptor signals to mitochondria. Cancer Biol Ther 2004;3:1051–1057. [PubMed: 15640619]
37. Guihard G, Bellot G, Moreau C, Pradal G, Ferry N, Thomy R, Fichet P, Meflah K, Vallette FM. The mitochondrial apoptosis-induced channel (MAC) corresponds to a late apoptotic event. J Biol Chem 2004;279:46542–46550. [PubMed: 15328340]
38. Verrier F, Deniaud A, Lebras M, Metivier D, Kroemer G, Mignotte B, Jan G, Brenner C. Dynamic evolution of the adenine nucleotide translocase interactome during chemotherapy-induced apoptosis. Oncogene 2004;23:8049–8064. [PubMed: 15377997]
39. Belzacq AS, Vieira HL, Verrier F, Vandecasteele G, Cohen I, Prevost MC, Larquet E, Pariselli F, Petit PX, Kahn A, Rizzuto R, Brenner C, Kroemer G. Bcl-2 and Bax modulate adenine nucleotide translocase activity. Cancer Res 2003;63:541–546. [PubMed: 12543814]
40. Kanno T, Sato EE, Muranaka S, Fujita H, Fujiwara T, Utsumi T, Inoue M, Utsumi K. Oxidative stress underlies the mechanism for Ca(2+)-induced permeability transition of mitochondria. Free Radic Res 2004;38:27–35. [PubMed: 15061651]
41. Fagian MM, Pereira-da-Silva L, Martins IS, Vercesi AE. Membrane protein thiol cross-linking associated with the permeabilization of the inner mitochondrial membrane by Ca2+ plus prooxidants. J Biol Chem 1990;265:19955–19960. [PubMed: 2123195]
42. Valle VG, Fagian MM, Parentoni LS, Meinicke AR, Vercesi AE. The participation of reactive oxygen species and protein thiols in the mechanism of mitochondrial inner membrane permeabilization by calcium plus prooxidants. Arch Biochem Biophys 1993;307:1–7. [PubMed: 8239645]
43. Bernardes CF, Meyer-Fernandes JR, Basseres DS, Castilho RF, Vercesi AE. Ca(2+)-dependent permeabilization of the inner mitochondrial membrane by 4,4′-diisothiocyanatostilbene-2,2′-disulfonic acid (DIDS). Biochim Biophys Acta 1994;1188:93–100. [PubMed: 7947908]
44. Lenartowicz E, Bernardi P, Azzone GF. Phenylarsine oxide induces the cyclosporin A-sensitive membrane permeability transition in rat liver mitochondria. J Bioenerg Biomembr 1991;23:679–688. [PubMed: 1917913]
45. Castilho RF, Kowaltowski AJ, Vercesi AE. The irreversibility of inner mitochondrial membrane permeabilization by Ca2+ plus prooxidants is determined by the extent of membrane protein thiol cross-linking. J Bioenerg Biomembr 1996;28:523–529. [PubMed: 8953384]

46. McStay GP, Clarke SJ, Halestrap AP. Role of critical thiol groups on the matrix surface of the adenine nucleotide translocase in the mechanism of the mitochondrial permeability transition pore. Biochem J 2002;367:541–548. [PubMed: 12149099]

47. Grasl-Kraupp B, Ruttkay-Nedecky B, Koudelka H, Bukowska K, Bursch W, Schulte-Hermann R. In situ detection of fragmented DNA (TUNEL assay) fails to discriminate among apoptosis, necrosis, and autolytic cell death: a cautionary note. Hepatology 1995;21:1465–1468. [PubMed: 7737654]

48. Ohno M, Takemura G, Ohno A, Misao J, Hayakawa Y, Minatoguchi S, Fujiwara T, Fujiwara H. “Apoptotic” myocytes in infarct area in rabbit hearts may be oncotic myocytes with DNA fragmentation: analysis by immunogold electron microscopy combined with In situ nick end-labeling. Circulation 1998;98:1422–1430. [PubMed: 9760297]

49. Kim JS, He L, Qian T, Lemasters JJ. Role of the mitochondrial permeability transition in apoptotic and necrotic death after ischemia/reperfusion injury to hepatocytes. Curr Mol Med 2003;3:527–535. [PubMed: 14527084]

50. Lemasters JJ, Qian T, Bradham CA, Brenner DA, Cascio WE, Trost LC, Nishimura Y, Nieminen AL, Herman B. Mitochondrial dysfunction in the pathogenesis of necrotic and apoptotic cell death. J Bioenerg Biomembr 1999;31:305–319. [PubMed: 10665521]

Abbreviations

ALD
: alcoholic liver disease

ANT
: adenine nucleotide translocator

GSH
: reduced glutathione

$\Delta\psi$
: mitochondrial membrane potential

MPT
: mitochondrial permeability transition

ROS
: reactive oxygen species

SOD1
: Cu, Zn-superoxide dismutase

***Sod1*$^{-/-}$c**
: *Sod1* knockout mice fed dextrose

***Sod1*$^{-/-}$e**
: *Sod1* knockout mice fed ethanol

***Sod1*$^{+/+}$c**
: -wild type mice fed dextrose

***Sod1*$^{+/+}$e**
: wild type mice fed ethanol

TUNEL
: terminal deoxynucleotidyl transferase–mediated dUTP nick-end labeling assay

UCP2
: uncoupling proteins 2

VDAC

voltage-dependent anion channel protein

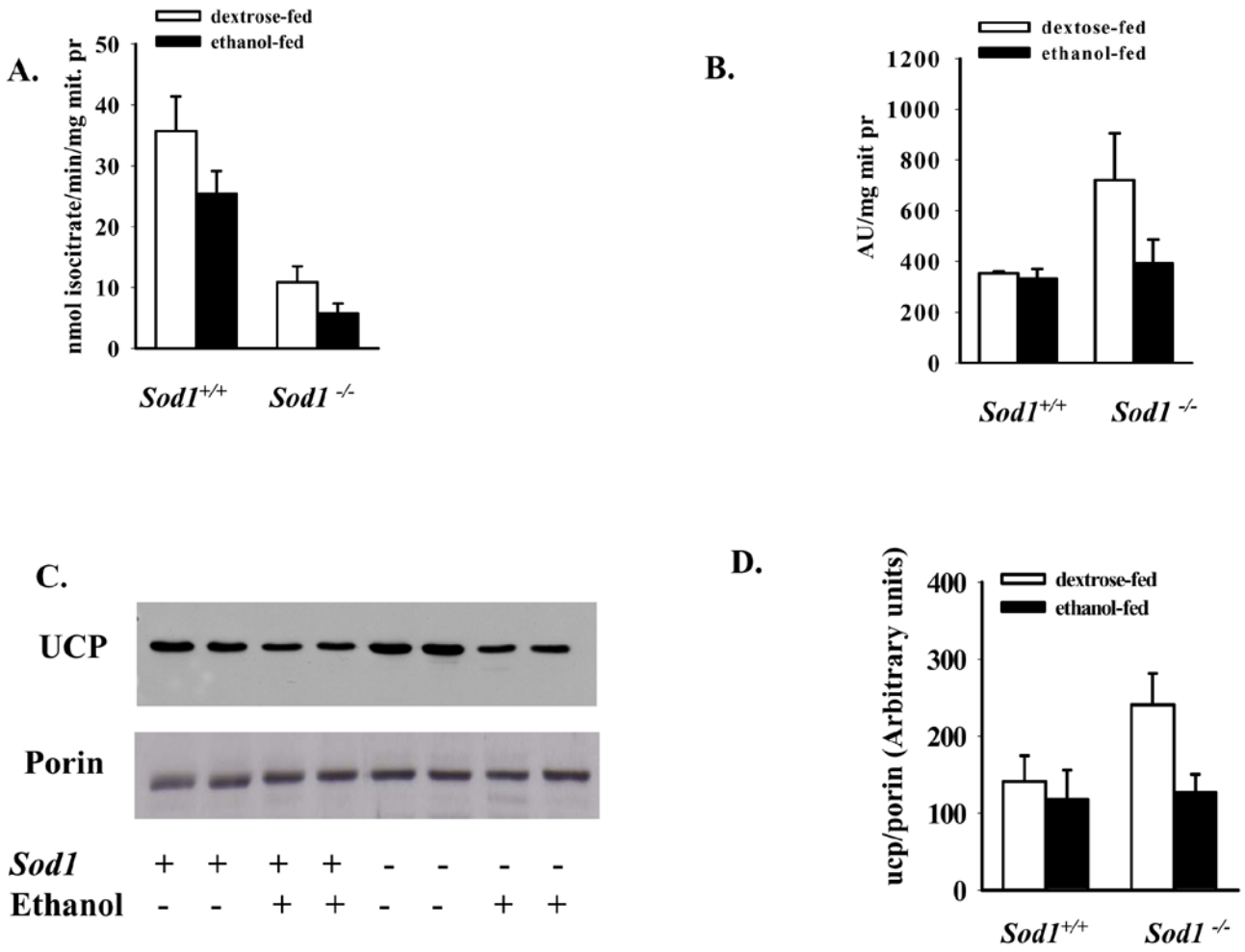

Figure 1. Effect of chronic ethanol consumption on aconitase activity (A), levels of total thiols (B) and content of uncoupling proteins (C, D) in isolated liver mitochondria of *Sod1*$^{+/+}$ and *Sod1*$^{-/-}$ mice

C. Representative Western blot of UCP2 content and porin levels in mitochondrial samples from 2 mice in each group, D. Quantification of the UCP2 content in mitochondria as detected by Western blots. The values represent the Mean ± SE of 4–6 mice. Effect of SOD deficiency and alcohol treatment were analyzed by two-way ANOVA.

A. Alcohol effect p=0.0037; SOD1 effect p=0.0012. B,D Alcohol effect p=0.033 and p=0.042 respectively.

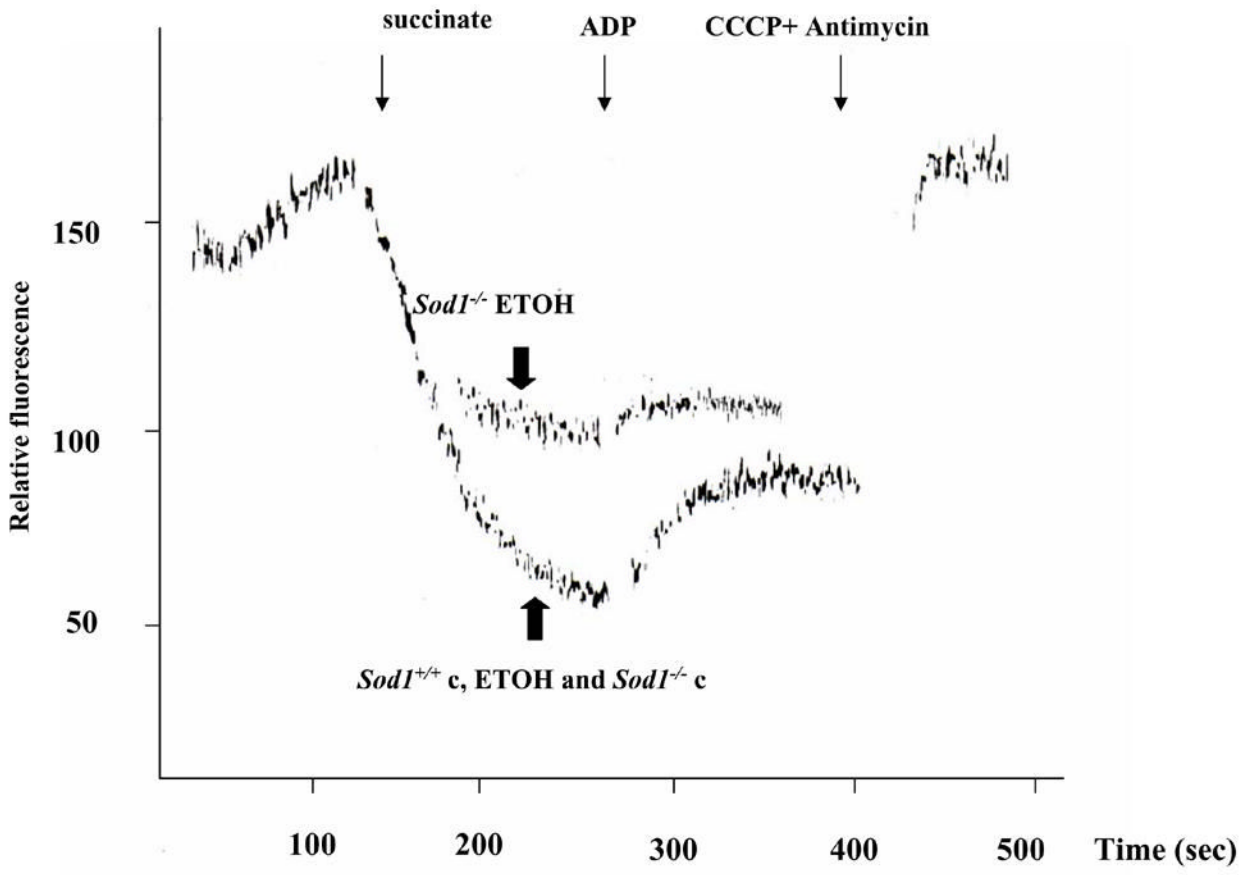

Figure 2. Decline in mitochondrial membrane potential in *Sod1* $^{-/-}$ mice-fed ethanol

Mitochondial energization was monitored by fluorescence quenching of Rh-123. Fluorescence with excitation at 503 nm and emission at 527 nm was measured in a reaction buffer containing 150 mM sucrose; 5 mM $MgCl_2$, 2.7 μM rotenone; 0.2 μM Rhodamine 123; 5 mM KPi buffer; 20 mM potassium-HEPES buffer, pH 7.4 and mitochondria (0.167mg/ml). Mitochondria were energized by addition of 5 mM disodium succinate (decrease in fluorescence) as respiratory substrate (State 4 respiration). Addition of 300 μM ADP causes an increase of fluorescence [quenching] (State 3 respiration). Mitochondria were deenergized with an uncoupler (1.3 μM CCCP) plus respiratory inhibitor (1.3 μg/ml antimycin). Each curve represents the Mean of 3–4 mice. *Sod1*$^{+/+}$c and *Sod1*$^{-/-}$c refer to the pair-fed wild type or *Sod1* knockout mice. The traces for the mitochondria from the wild type mice fed dextrose or ethanol and from the SOD1 knockout mice fed dextrose are virtually identical and are overlaid on top of each other for all conditions (succinate, ADP, CCCP plus antimycin).

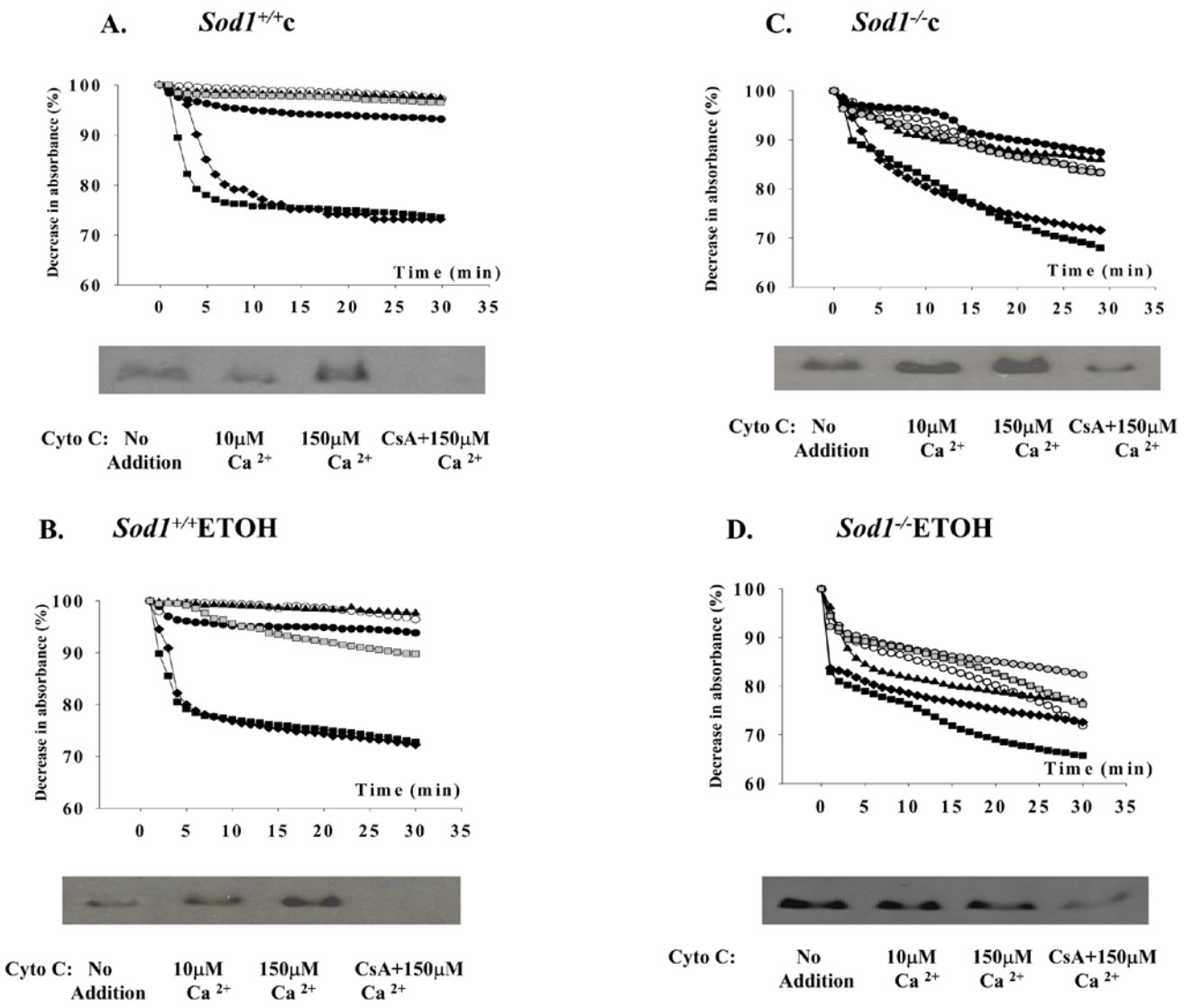

Figure 3. Chronic ethanol consumption intensifies the mitochondrial permeability transition (MPT) and cytochrome C release from mitochondria of *Sod1* $^{-/-}$ mice

For MPT determination, mitochondria (0.5mg/ml) were incubated in respiration buffer at 25° C as described in *Materials and Methods*. Swelling was monitored for 30 min at 540 nm in mitochondria (○); mitochondria plus respiratory substrates 1 mM glutamate and 1mM malate without calcium (●); with 10 μM $CaCl_2$ (▲); with 50 μM $CaCl_2$ (◆), or with 150 μM $CaCl_2$ (■). 2 μM cyclosporin A was added to mitochondria before incubation with (□) or without (○) 150 μM Ca to prevent MPT. Each curve represents the Mean of 3–4 mice

For cytochrome C release to the incubation medium, mitochondria (1 mg/ml) were incubated for 15 min at 25 °C in respiration buffer with the indicated additions. The reaction mixtures were then centrifuged at 9,000 × g for 10 min at 4 °C and supernatant was concentrated by ultrafiltration through Centrikon 10 membranes (Amicon) at 4 °C. The concentrated supernatants were subjected to SDS-PAGE and analyzed by Western blotting using anti-cytochrome c antibody. Results show the cytochrome c present in the concentrated supernatants obtained after mitochondria from the 4 groups were incubated with no addition, or 10 uM calcium, or 150 uM calcium or 150 uM calcium plus 2 uM cyclosporin A.

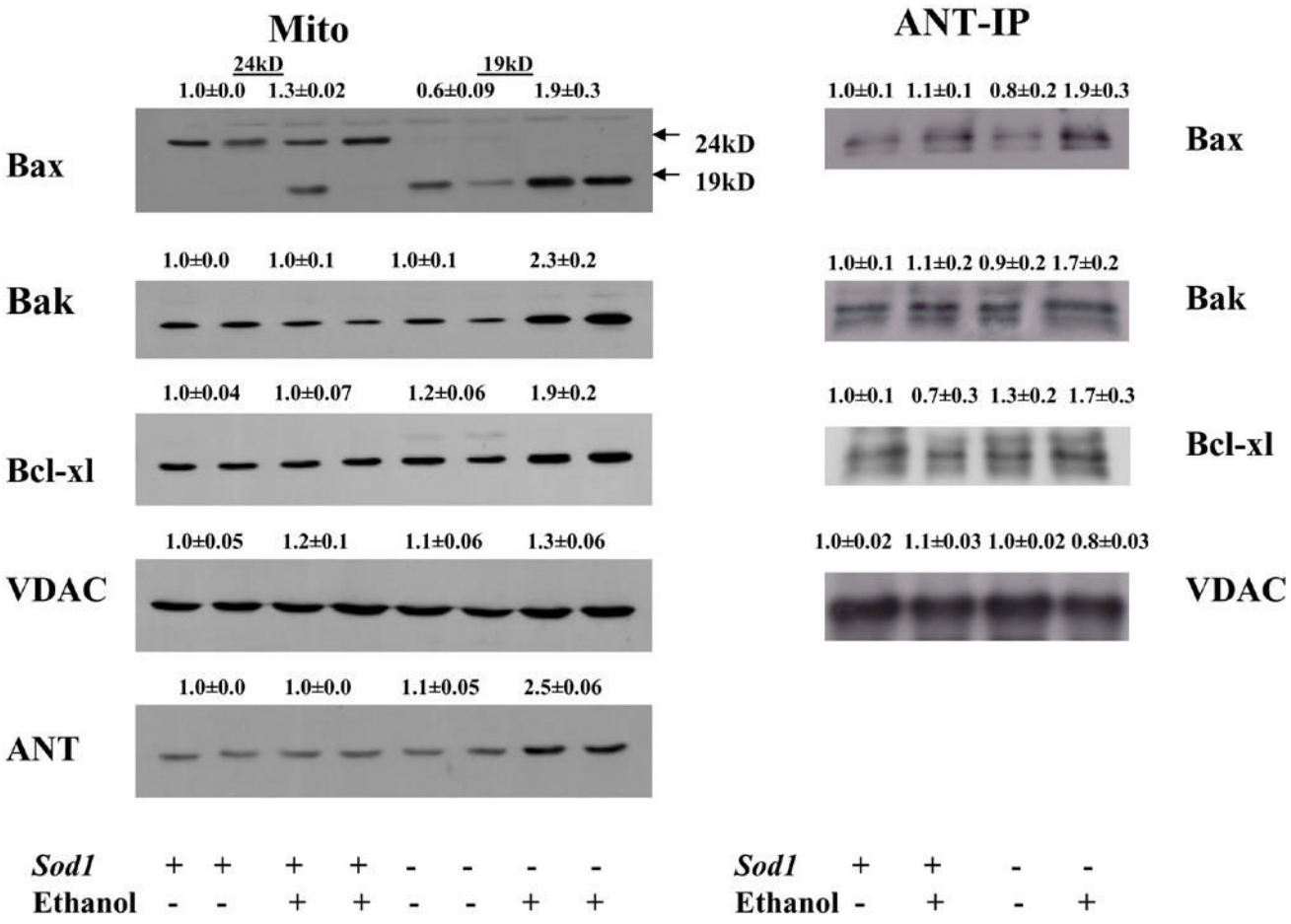

Figure 4. Expression of MPT pore components and their interactions in mitochondria of *Sod1*$^{+/+}$ and *Sod1*$^{-/-}$ mice

A. Western blotting was conducted with 100 μg mitochondrial protein using anti-Bax, anti-Bak, anti-Bcl-xl, anti-VDAC and anti-ANT antibodies. B. Isolated mitochondria were subjected to immunoprecipitation with an ANT specific antiserum as described in *Materials and Methods.* Equal amounts of precipitated ANT proteins, estimated by Western blot, were loaded for SDS-PAGE and protein interactions were detected by using the corresponding anti-Bax, anti-Bak, anti-Bcl-xl and anti-VDAC antibodies

Each immunoblot has been reproduced at least from three mice. Numbers above the blots refer to arbitrary densitometric units with results for the pair-fed wild type mice taken as 1.0.. Effects of SOD1 deficiency and alcohol treatment were analyzed by two-way ANOVA. Ethanol effect on ANT content p=0.003. Effect of SOD1 deficiency on Bax, Ant and ANT-Bax content p=0.0001;p=0.004, p=0.044 respectively; interaction p=0.0062; p=0.005; p=0.031 respectively. One way ANOVA followed by Student-Newman-Keul posthoc test indicated that the increase in Bax, Bak, Bclxl, ANT and the ANT-Bax and ANT-Bak comples was statistically significant (<0.05) as compared to the 3 other groups.

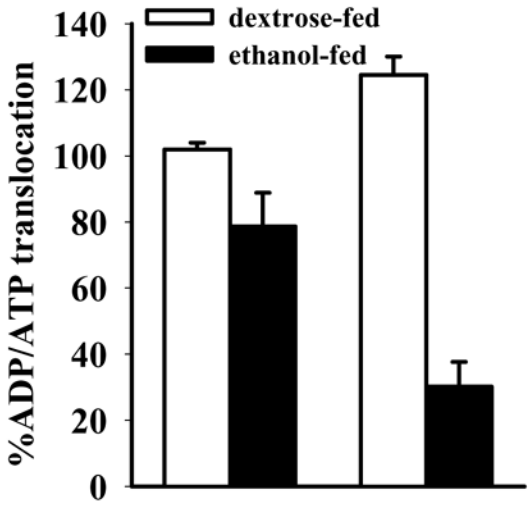

Figure 5. Decrease in ATP/ADP exchange in isolated mitochondria from *Sod1* $^{-/-}$ mice

Isolated mitochondria (7 mg/500 μl buffer) were loaded with [^{3}H]-labeled ATP. The exchange was initiated by addition of cold 400 μM ADP and stopped by addition of 100 μM atractyloside after 10 sec. The reaction mixture was centrifuged at 9,000 × g for 10 min at 4 °C and the supernatant and mitochondrial pellets were subjected to scintillation counting. ATP release into the mitochondrial supernatant was measured and expressed as a percentage of [^{3}H] counts compared to [^{3}H]counts in mitochondria with the results for the mitochondria from the *Sod1*$^{+/+}$ mice-fed dextrose taken as the 100% value. Effects of SOD1 deficiency and alcohol treatment were analyzed by two-way ANOVA. Alcohol effect p=0.005; SOD1 effect p= 0.023; interaction p=0.0008.

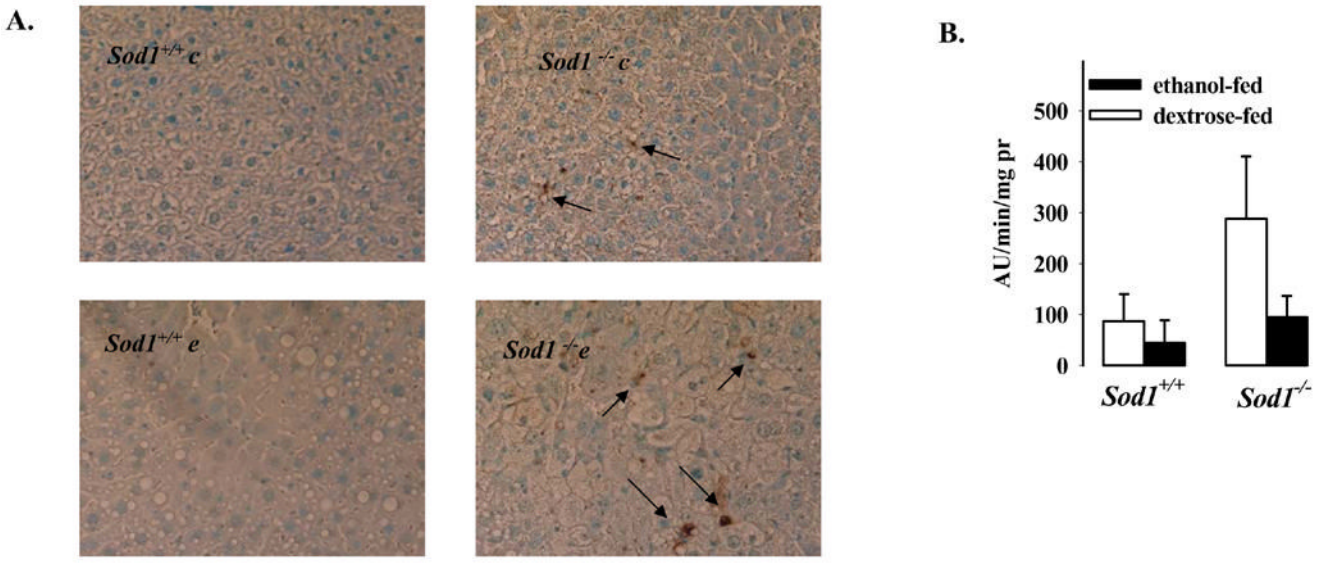

Figure 6. Effect of chronic ethanol consumption on DNA fragmentation and activity of caspase 3 in livers of *Sod1* $^{-/-}$ mice

DNA fragmentation was determined by the TUNEL assay as described in Materials and Methods (A). Caspase 3 activity in hepatic cytosols was assayed using 50 μM Ac-DEVD-AMC fluorogenic peptide as substrate (B). The released AMC was determined fluorometrically and results expressed as arbitrary units of fluorescence per min per mg cytosolic protein. Effect of alcohol feeding on caspase 3 activity p=0.0039 by two-way ANOVA.

Table 1

Effect of Chronic Ethanol Feeding on Glutamate plus Malate and Succinate-Dependent Oxygen Consumption in Liver

	***Sod1*$^{+/+}$c**	***Sod1*$^{+/+}$e**	***Sod1*$^{-/-}$c**	***Sod1*$^{-/-}$e**
state 4 (glutamate-malate)	0.017 ± 0.001	0.012 ± 0.000	0.013 ± 0.001	0.022 ± 0.001*
state 3 (glutamate-malate)	0.085 ± 0.045	0.065 ± 0.010	0.064 ± 0.009	0.057 ± 0.005
RCR (glutamate-malate)	4.95 ± 0.45	4.40 ± 0.55	4.97 ± 0.58	2.63 ± 0.24**
P/O (glutamate-malate)	2.36 ± 0.33	2.53 ± 0.15	2.71 ± 0.63	1.49 ± 0.03$^{\#}$
state 4 (succinate)	0.034 ± 0.005	0.024 ± 0.004	0.025 ± 0.003	0.036 ± 0.003$^{\#\#}$
state 3 (succinate)	0.110 ± 0.003	0.072 ± 0.004	0.080 ± 0.015	0.092 ± 0.008$^{\#\#}$
RCR (succinate)	3.63 ± 0.50	3.06 ± 0.28	2.93 ± 0.29	2.56 ± 0.03
P/O (succinate)	1.88 ± 0.17	2.1 ± 0.12	1.62 ± 0.31	1.43 ± 0.32

Respiratory rates were assessed by measuring the oxygen consumption of mitochondria using Clark-type electrodes. Mouse liver mitochondria (0.8mg/ml) were incubated in respiration buffer at pH 7.4 at 30°C in the presence of 5 mM malate/5mM glutamate or succinate in the absence (State 4) or presence (State 3) of 0.3 mM ADP. Rates refer to uatoms O_2 consumed per min per mg mitochondrial protein.

Effects of sod1 deficiency and alcohol treatment were analyzed by two-way ANOVA.

*Alcohol effect p=0.04, sod1 effect p=0.015;interaction p=0.0029;

**sod1 effect p=0.0075;

$^{\#}$Interaction p=0.044

$^{\#\#}$Interaction p=0.05